Study of Polymers for the Implementation of an Axial Impeller with a Central Shaft in a Ventricular Assist Device

Johanna Muñoz-Pérez[1,3] [a], Carlos Jiménez-Carballo[2] [b], Gabriela Ortiz-León[3] [c]
and Marta Vílchez-Monge[3] [d]

[1]*Master Program in Medical Devices Engineering, School of Materials Science and Engineering,*
Instituto Tecnológico de Costa Rica, Cartago, Costa Rica
[2]*School of Physics, Instituto Tecnológico de Costa Rica, Cartago, Costa Rica*
[3]*Academic Area of Mechatronics Engineering, Instituto Tecnológico de Costa Rica, Cartago, Costa Rica*

Abstract: The main goal of the present research was to determine the value of the mechanical parameters with which a material to be used in a blood pump impeller must comply. To obtain these values, multiphysical numerical simulation and modeling of the Fluid-Structure Interaction (FSI) of the impeller with defined conditions and geometry was carried out, by means of Computational Fluid Dynamics (CFD) based on the Finite Element Method (FEM), specifically the partitioned procedure was used. As a result of the simulations, the deformed geometries, the maximum values of the Von Mises stress and the volumetric deformations for an axial impeller with a central shaft were obtained. From this research it was determined that from the structural point of view the selected biocompatible polymers are candidates for the manufacture of the impeller.

1 INTRODUCTION

In 2011 began the development of a ventricular assist device (VAD) at the Instituto Tecnológico de Costa Rica (TEC) (Ortiz-León et al., 2012), (Ortiz, 2017), (Ortiz-León et al., 2014). Previous research reveals that the main drawback of introducing a blood pump into the body of a living being, are the adverse effects that this device causes in the blood fluid, that is, hemolysis and thrombosis (Tchantchaleishvili et al., 2014) that could be related to the materials used in the manufacture of the impeller.

On the other hand, increasing the lifespan of the device is an important goal in order to extend the time a person can carry it implanted before reaching a critical condition. Any improvement in the performance of a blood pump in terms of avoiding these adverse effects represents a significant advance from the point of view of the patient and the economic cost of maintaining the device.

The main goal of this research is to determine the value of the mechanical parameters that the material to be used in a blood pump impeller must meet. Specifically, it is desired to introduce the fluid structure interaction model to the mathematical modeling of the impeller, in order to visualize the effect that the operation of the impeller has on the structure itself. In other words, it seeks to determine the distribution of stresses and deformations due to the fluid-structure interaction and then to determine the ranges of deformation and mechanical resistance that do not compromise the functionality of the impeller. Finally, based on the above, it is desired to determine a list of biocompatible polymers whose mechanical characteristics are within the required ranges.

Therefore, this document is structured as follows: in section 2 a description and list of biocompatible materials is presented, in section 3 the failure criteria used are explained, in section 4 the methodology used for the fluid-structure interaction of the impeller is mentioned, in section 5 the results obtained by means of simulation are presented including the visualization of the points subjected to greater stress and finally, conclusions about the pertinency in the use of the studied materials for the desired application are obtained.

[a] https://orcid.org/0000-0003-1778-414X
[b] https://orcid.org/0000-0003-1783-3159
[c] https://orcid.org/0000-0002-0940-2677
[d] https://orcid.org/0000-0002-3271-2569

2 BIOCOMPATIBLE POLYMERS

The FDA defines a medical device as "an implant, intended for use in the mitigation, treatment, or prevention of disease, and which does not achieve its primary intended purposes through chemical action" (FDA, 2018). An implant or device must be able to maintain its functionality within the biological environment of the body, complying with chemical, mechanical, electrical or thermal requirements.

The biocompatibility of a material is defined in simple terms as its ability not to cause adverse effects on body tissues. Achieving an adequate host response due to interaction with a material involves identifying and characterizing tissue reactions and adverse responses that could lead to the failure of the biomaterial, medical device or prosthesis. The assessment of biocompatibility is considered a measure of the magnitude and duration of adverse alterations that determine host response (Anderson, 2012).

Biomaterials are prepared using metals, ceramics and polymers. Ceramics have good biocompatibility, corrosion resistance, compressive strength and high density. Some disadvantages of ceramics include its fragility, low fracture resistance, low mechanical reliability, and complicated manufacturing processes. Metals have high ductility, wear resistance and high density. Polymers can be easily manufactured in complex shapes and structures, however they do not always meet the mechanical requirements of the application while sterilization processes could affect the properties of the polymer (Teo et al., 2016) (Clavería and Puértolas, 2011).

For this research, the studied polymers are listed bellow:

1. **TECAPEEK:** Polyetheretherketone
2. **PC:** Polycarbonate
3. **PMMA:** Polymethyl Methacrylate
4. **PP:** Polypropylene
5. **UHMW-PE:** Ultra High Molecular Weight Polyethylene

Table 1 shows the values required to perform the structural simulations of the different materials: Young's modulus (E), elastic limit (σ_Y), density (ρ) and Poisson ratio (ν). These values are obtained from the corresponding data sheets of each material, considering that a medical use spectrum was selected for each type of polymer and if possible where its application in implantable devices is indicated (Teo et al., 2016), (Matarneh et al., 2018).

Table 1: Mechanical properties of the selected polymers.

Material	E (GPa)	σ_Y (MPa)	ρ (kg/m^3)	ν
Tecapeek (Ensinger, 2020)	4.4	117	1400	0.40
PC (Sabic, 2020)	2.3	60	1200	0.37
PMMA (Campus, 2020)	1.6	31	1090	0.36
PP (Ensinger, 2017b)	1.45	35	920	0.43
UHMW-PE (Ensinger, 2017a)	0.66	22.2	936	0.46

3 MATERIALS FAILURE CRITERIA

If external forces are applied to a deformable body, internal forces try to counteract these external forces. The simplest way to analyze these internal forces and the deformation generated by external forces on the body is through the concept of stress τ_{ij} (James, 2004).

If a body is sectioned in several planes parallel to the coordinate axes, it is possible to obtain a volume element where the state of the different stresses is represented. In this way the volume element has three components of stress that act on each of its faces. The nine components of the volume element stress make up the second-order stress tensor σ. This tensor is presented in equation 1. Also, if an infinitesimal element is considered to be unable to transfer moments, then $\tau_{ij} = \tau_{ji}$, implying that the tensor is symmetric (Rosler et al., 2007).

$$\sigma = \begin{pmatrix} \sigma_{xx} & \tau_{xy} & \tau_{xz} \\ \tau_{yx} & \sigma_{yy} & \tau_{yz} \\ \tau_{zx} & \tau_{zy} & \sigma_{zz} \end{pmatrix} = \begin{pmatrix} \sigma_{11} & \sigma_{12} & \sigma_{13} \\ \sigma_{21} & \sigma_{22} & \sigma_{23} \\ \sigma_{31} & \sigma_{32} & \sigma_{33} \end{pmatrix} \quad (1)$$

For metallic materials, the von Mises failure criterion is normally used. First, an equivalent stress is defined and compared to the critical stress or elastic limit of the material (σ_Y). If the equivalent von Mises stress σ_v is greater than the critical stress σ_Y, the metal material is considered to fail. From the normal stresses (σ_{ii}) and the shear stresses (σ_{ij}), this failure criterion can be expressed as (Ugural and Fenster, 2011)

$$\sigma_v = \sqrt{\frac{1}{2}\sigma_a^2 + 3\left(\sigma_{23}^2 + \sigma_{13}^2 + \sigma_{12}^2\right)} \geq \sigma_Y, \quad (2)$$

with

$$\sigma_a^2 = (\sigma_{11} - \sigma_{22})^2 + (\sigma_{22} - \sigma_{33})^2 + (\sigma_{11} - \sigma_{33})^2. \quad (3)$$

For any stress tensor there is a coordinate system where only the diagonal components of the tensor remain, while all parts outside the diagonal become zero. In this coordinate system, all stresses are normal and are called the principal stresses of the stress tensor. The axes of the coordinate system are called principal axes and the principal stresses are denoted by Arabic numbers: $\sigma_1 \geq \sigma_2 \geq \sigma_3$. The diagonalized stress tensor is presented in equation 4 (Rosler et al., 2007).

$$\sigma_{diagonalized} = \begin{pmatrix} \sigma_1 & 0 & 0 \\ 0 & \sigma_2 & 0 \\ 0 & 0 & \sigma_3 \end{pmatrix} \quad (4)$$

Using the principal stresses (σ_1, σ_2 and σ_3) the failure criterion is expressed as

$$\sigma_v = \sqrt{\frac{1}{2}\left[(\sigma_1 - \sigma_2)^2 + (\sigma_1 - \sigma_3)^2 + (\sigma_2 - \sigma_3)^2\right]} \geq \sigma_Y, \quad (5)$$

For polymeric materials and ceramics, the failure criterion establishes that the principal stresses σ_i ($i = 1, 2, 3$) are greater than σ_Y or σ_{UTS} (Ultimate Tensile Strength for ceramics) (Mayorga-Espinoza, 2018).

$$1 \gg \frac{\sigma_Y}{\sigma_i}. \quad (6)$$

4 METHODOLOGY

A literature review shows that the main strategies used for solving Fluid-Structure Interaction (FSI) problems are (Rugonyi and Bathe, 2001), (Pedro and Sibanda, 2012):

- *Simultaneous procedure* in which the complete system is solved as a single entity, which means that the equations of fluid mechanics and those of structural mechanics are solved simultaneously (Park et al., 1977).

- *Partitioned or iterative procedure* where the solution of the process is developed in stages, for example first the fluid field (or the structural one) is solved and with the obtained solution the second field is solved. Later with these solutions the first field is solved again, and thus it is continued iteratively until convergence is reached (Farhat and Lesoinne, 2000).

Initially, the integration of the fluid and the structure was proposed to simulate simultaneously the deformation experienced by the geometry under study and the modifications that this new deformed geometry caused in the fluid. However, the computational resources of this approach are very demanding, so it was necessary to divide the study into two simulations (Mayorga-Espinoza, 2018).

Therefore, in this research the second procedure is used as follows: first it begins with the resolution of the equations of *Navier-Stokes* which allows to obtain the velocity fields, the pressure fields and other hydrodynamic quantities. These results are then used as boundary conditions in the deformable structure to obtain stresses, velocities, accelerations and deformations of the solid body. The process described to achieve fluid-structure interaction is shown in figure 1 (Muñoz-Pérez, 2021).
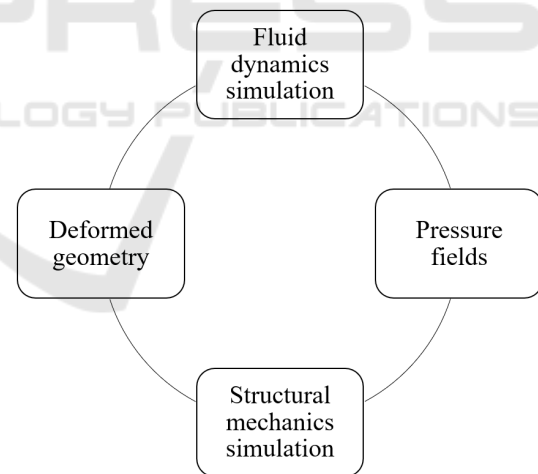

Figure 1: Fluid-structure interaction process.

5 RESULTS

5.1 Fluid Simulations

As indicated in section 4, the strategy used to solve the FSI problem posed in this research is the *partitioned procedure*, this is because it was considered that the impellers only suffer small deformations . It

is important to note that simulations were developed with the help of the COMSOL Multiphysics® program.

During the development of the partitioned method, the results obtained from the fluid simulation carried out in (Ortiz, 2017) on the geometry and pressure fields for a rotational speed ω of 10500 rpm (Reul and Akdis, 2000), (Song et al., 2003) and four output speeds of the blood v (0.25 m/s, 0.50 m/s, 0.75 m/s and 1.00 m/s) were used. The behavior of blood was modeled using a Newtonian, incompressible and k-ε turbulence flow model, with a dinamic viscosity of 0.0035 Pa·s and a density of 1052.82 kg/m^3.

Boundary conditions of pressure and velocity were used at the impeller inlet and outlet, respectively. The pressure diference between the inlet and outlet of the impeller is 40 mmHg. To simulate continuity condition between the fixed and rotational domain interface, the continuity boundary condition was used (Ortiz, 2017). Figure 2 shows the graph of the pressure distribution in the impeller structure for the case where the rotational speed ω is 10500 rpm and the blood output speed v is 1.00 m/s.

The pressure distribution in figure 2 shows that the greatest pressure is obtained in the section of the blades of both the impeller and the diffuser. In addition, the diffuser shaft has a greater pressure difference compared to the impeller and infuser shaft. Zones with negative pressures correspond to regions where the fluid moves faster.

5.2 Structural Simulations

Next, the structural simulations were carried out where the results of the mentioned pressure fields were used as boundary conditions in a deformable solid model of the selected program, this is to simulate the steady state condition of the impeller. At the same time, the impellers were subjected to the oscillating load characteristic of the pulsations of the system according to the cardiac cycle equation (Araya-Luna, 2012).

The results of the simulations are presented in table 2 where t is the time in which the greatest volumetric deformation is reached, σ_i is the principal stress, p is the highest surface pressure, d_M is the maximum displacement, ε_V is the unit volumetric deformation and σ_Y/σ_i is the ratio between the elastic limit and the principal stress. These simulations were run with a time-dependent study for four seconds, which is equivalent to four cardiac cycles.

Based on table 2 the maximum displacements of a point in the geometry d_M are in the order of magnitude of μm. Besides, it was found that the maximum unit

volumetric deformation ε_V is equal to 28.649×10^{-5} for UHMW-PE and the minimum value is equal to 6.7379×10^{-5} for Tecapeek. Both parameters are negigible compared to the dimensions of the structure.

On the other hand, the relationship σ_Y/σ_i shown in table 2 all materials meet the design criteria since the relationship between their elastic limit and principal stress for any v is greater than 10. Regarding the relationship σ_Y/σ_i, it is found that Tecapeek is the most resistant material, which is explained because it has the highest Young's modulus of 4.4 GPa. It is also observed that a Young's modulus around 0.66 GPa seems potentially suitable for the impeller application. Table 2 shows that the UHMW-PE for an output speed v of 0.25 m/s has the lowest ratio σ_Y/σ_i, that is, the highest structural stress.

The von Mises stresses and deformed geometry in the impeller with a central shaft using UHMW-PE for an output velocity v of 0.25 m/s are shown in Figure 3, in which it can be seen that there is no significant difference between the deformed surface and the undeformed surface. It is evident from figure 3 that for the entire structure the stresses of the greatest magnitude are concentrated in the diffuser blades that are located towards the output. Figure 4 shows a *ZY* view where the stresses in the diffuser can be seen in greater detail, in which the surface in red color corresponds to the attack area of the moving fluid. According with both figures, the maximum von Mises stress of 0.492 MPa is lower than the σ_Y for this material (table 1), which implies that this structure meets the design criteria as established by equation 5.

In agreement with the results obtained from the simulations carried out, it is clear that the polymers used are suitable for the construction of an impeller with a central shaft, at least from the structural point of view.

6 CONCLUSIONS

This paper presents the mechanical properties for five biocompatible polymers to be used in a blood pump impeller. These includes the deformed geometries, the maximum values of the Von Mises stress and the volumetric deformations for the axial impeller with a central shaft.

Firstly, a *partitioned* mathematical model was developed for the fluid-structure interaction in a blood pump impeller and also the ranges of values were established for the variables that the fluid requests from the material for the type of impeller studied in this research.
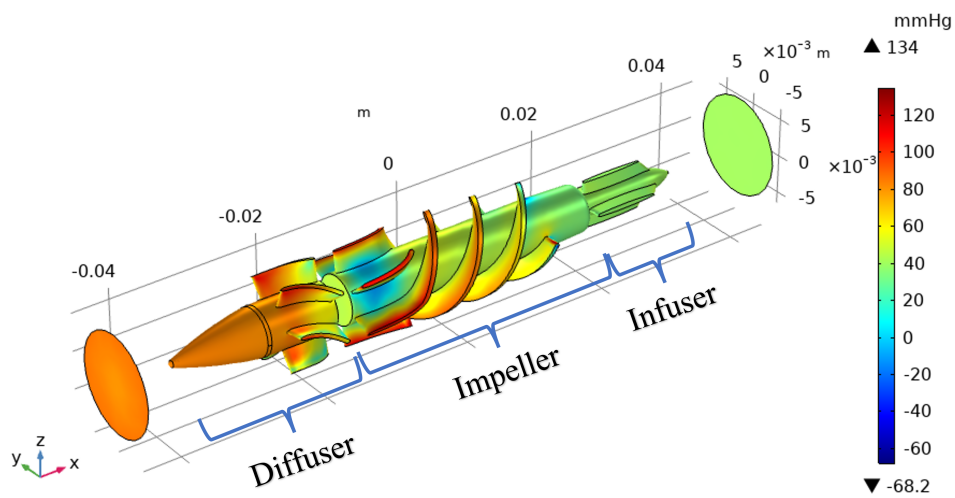
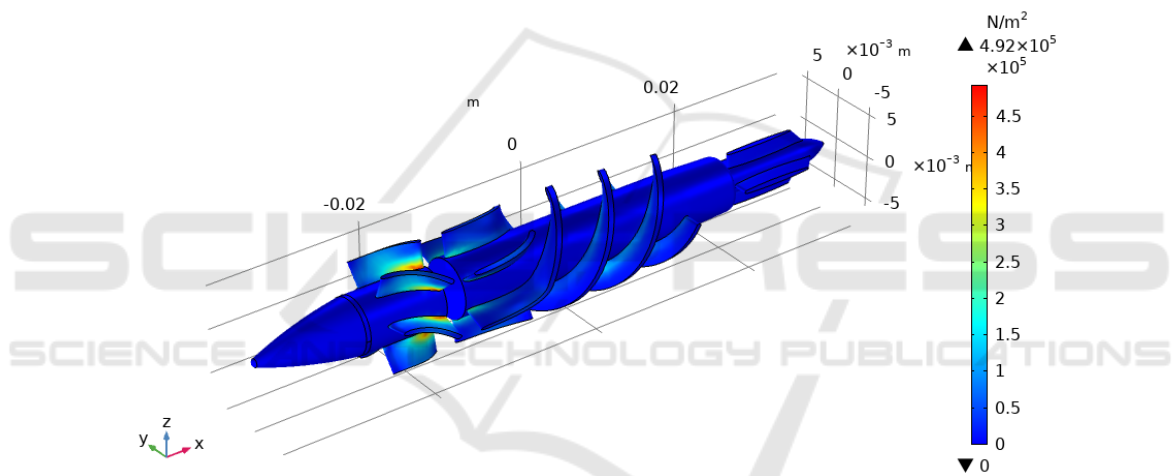Figure 2: Pressure field for ω = 10500 rpm (clockwise) and v = 1.00 m/s ($-x$ direction).

Figure 3: Von Mises stress on the UHMW-PE material for ω = 10500 rpm and v = 0.25 m/s (isometric view).
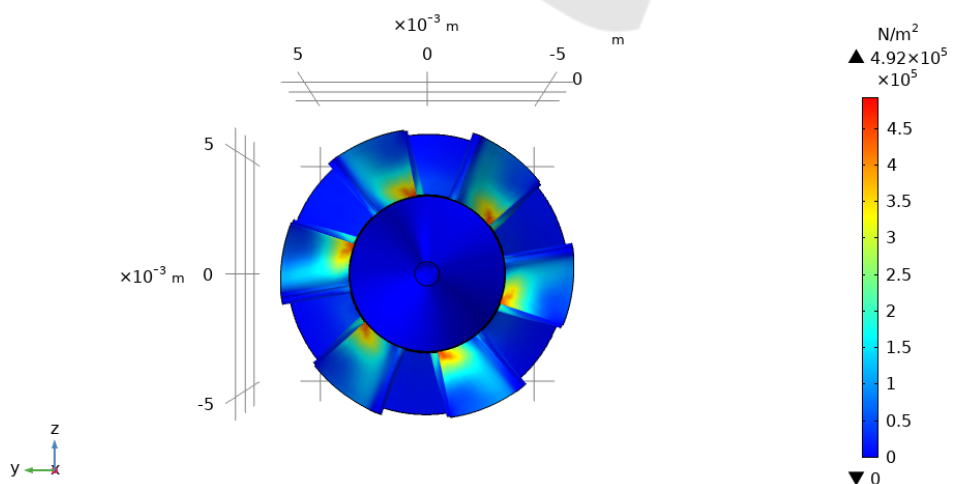

Figure 4: Von Mises stress on the UHMW-PE material for ω = 10500 rpm and v = 0.25 m/s (ZY view).

Table 2: Results of the structural simulations for the five selected polymers with $\omega = 10500$ rpm of an impeller with a central shaft, and different v.

v (m/s)	Material	t (s)	σ_i (MPa)	p (MPa)	d_M (μm)	ε_V ($\times 10^{-6}$)	σ_Y/σ_i
1.00	Tecapeek	0.0	0.77245	0.52748	0.39591	72.226	151
	PC	3.9	0.66055	0.38443	1.2830	144.97	90
	PMMA	4.0	0.65195	0.37385	1.8557	217.06	47
	PP	4.0	0.73668	0.48078	1.9395	157.95	47
	UHMW-PE	2.9	0.85477	0.64944	4.1345	258.31	25
0.75	Tecapeek	0.0	0.75024	0.51608	0.34470	70.236	155
	PC	3.9	0.63450	0.43873	1.2281	137.70	94
	PMMA	4.0	0.63072	0.42561	1.7783	206.36	49
	PP	3.9	0.71975	0.51334	1.8243	154.66	48
	UHMW-PE	1.8	0.79739	0.61806	3.8020	233.58	27
0.50	Tecapeek	4.0	0.74566	0.63792	0.79691	67.379	156
	PC	2.9	0.81767	0.53219	1.5614	179.64	73
	PMMA	2.0	0.79258	0.53728	2.2634	249.68	39
	PP	3.0	0.83444	0.72343	2.3327	168.74	41
	UHMW-PE	3.6	0.84565	0.89118	4.8891	243.75	26
0.25	Tecapeek	2.9	0.82486	0.75352	0.92138	74.960	141
	PC	4.0	0.89698	0.67423	1.8104	186.91	66
	PMMA	3.0	0.88899	0.65058	2.6198	281.05	34
	PP	3.9	0.95103	0.88347	2.7190	193.00	36
	UHMW-PE	2.8	0.99362	1.0715	5.7153	286.49	22

Subsequently, it was determined that the unit volumetric deformation (ε_V) represents a negligible value for practical purposes, this is because its value has an order of magnitude between 10^{-5} and 10^{-4}. Additionally, it was found that the order of magnitud for the maximum displacement (d_M) is also negigible since it is around μm.

During research development, a limit safety factor of 10 was established represented by the ratio σ_Y/σ_i evidenced in table 2. From this factor it was determined that the following biocompatible polymers are candidates, from the structural point of view, for the manufacture of the impeller:

1. **TECAPEEK:** Polyetheretherketone
2. **PC:** Polycarbonate
3. **PMMA:** Polymethyl Methacrylate
4. **PP:** Polypropylene
5. **UHMW-PE:** Ultra High Molecular Weight Polyethylene

Finally, each of these materials has a version for industrial use and another for medical grade, so a careful selection of the material with which physical tests will be implemented is required. In addition, it is recommended that the experimental tests carried out

should include the determination of the mechanical properties obtained from the datasheets, to contrast that information with the one provided by the manufacturer.

ACKNOWLEDGEMENTS

REFERENCES

Anderson, J. (2012). *Polymer science: a comprehensive reference. Amsterdam.* Oxford, Waltham: Elsevier.

Araya-Luna, D. (2012). Modelado de la interacción del fluido sanguíneo sometido a presión pulsátil en la unión de un conducto arterial y un conducto rígido (p. 140).

Campus (2020). Cyrolite Med 2 PMMA. [Online]. Available: https://www.campusplastics.com/campus/es/datasheet/CYROLITE%C2%AE+Med+2/R%C3%B6hm+GmbH/21/c535b7c0.

Clavería, J. and Puértolas, J. A. (2011). Implantes biomédicos. Master's thesis.

Ensinger (2017a). Chirulen 1020 UHMW-PE. [Online]. Available: https://www.mcam.com/na-en/products/meditechr-life-science-grade/implantable-polymers/?r=1#c32789.

Ensinger (2017b). Tecapro MT Black PP. [Online]. Available: https://www.ensingerplastics.com/es-br/semielaborados/plastico/pp-de-grado-medico-tecapro-mt-black.

Ensinger (2020). Tecapeek MT Classix white PEEK. [Online]. Available: https://www.ensingerplastics.com/es-br/semielaborados/plastico/peek-de-grado-medico-tecapeek-mt-classixtm-white-.

Farhat, C. and Lesoinne, M. (2000). Two efficient staggered algorithms for the serial and parallel solution of three-dimensional nonlinear transient aeroelastic problems. *Computer methods in applied mechanics and engineering*, 182(3-4):499–515.

FDA (2018). Medical device overview. [Online]. Available: https://www.fda.gov/industry/regulated-products/medical-device-overview.

James, G. M. (2004). *Mechanic of Materials, Sixth Edition.* Thomson Learning.

Matarneh, R., Sotnik, S., and Lyashenko, V. (2018). Polymers in cardiovascular surgery.

Mayorga-Espinoza, C. (2018). Determinación computacional del comportamiento fluido-estructura de un impulsor en flujo sanguíneo. Master's thesis.

Muñoz-Pérez, J. (2021). Determinación computacional de la fatiga en un impulsor axial sin eje central en flujo sanguíneo. Master's thesis.

Ortiz, G. (2017). *Modelo de un nuevo concepto de impulsor para la aplicación en bombas de sangre*. PhD thesis.

Ortiz-León, G., Araya-Luna, D., and Vílchez-Monge, M. (2014). Revisión de modelos teóricos de la dinámica de fluidos asociada al flujo de sangre. *Revista Tecnología en Marcha*, 27(1):66–76.

Ortiz-León, G., Coto-Cortés, A., Vílchez-Monge, M., Salazar, C., Campos, G., Varela, F., Araya-Luna, D. E., Li-Huang, L. A., and Montero-Rodríguez, J. J. (2012). Estudio exploratorio para el desarrollo de un dispositivo de asistencia cardíaca.

Park, K., Felippa, C., and DeRuntz, J. (1977). Stabilization of staggered solution procedures for fluid-structure interaction analysis. *Computational methods for fluid-structure interaction problems*, 26(94-124):51.

Pedro, J. C. and Sibanda, P. (2012). An algorithm for the strong-coupling of the fluid-structure interaction using a staggered approach. *International Scholarly Research Notices*, 2012.

Reul, H. M. and Akdis, M. (2000). Blood pumps for circulatory support. *Perfusion*, 15(4):295–311.

Rosler, J., Harders, H., and Baker, M. (2007). *Mechanical behaviour of engineering materials, 1st edition*, volume 3. Berlin et al.: Springer-Verlag.

Rugonyi, S. and Bathe, K.-J. (2001). On finite element analysis of fluid flows fully coupled with structural interactions. *CMES- Computer Modeling in Engineering and Sciences*, 2(2):195–212.

Sabic (2020). Lexan Healthcare Resin HPS6 PC. [Online]. Available: https://www.sabic.com/en/products/polymers/polycarbonate-pc/lexan-healthcare-resin.

Song, X., Throckmorton, A. L., Untaroiu, A., Patel, S., Allaire, P. E., Wood, H. G., and Olsen, D. B. (2003). Axial flow blood pumps. *ASAIO journal*, 49:355–364.

Tchantchaleishvili, V., Sagebin, F., Ross, R. E., Hallinan, W., Schwarz, K. Q., and Massey, H. T. (2014). Evaluation and treatment of pump thrombosis and hemolysis. *Annals of cardiothoracic surgery*, 3(5):490.

Teo, A. J., Mishra, A., Park, I., Kim, Y.-J., Park, W.-T., and Yoon, Y.-J. (2016). Polymeric biomaterials for medical implants and devices. *ACS Biomaterials Science & Engineering*, 2(4):454–472. doi: 10.1021/acsbiomaterials.5b00429.

Ugural, A. C. and Fenster, S. K. (2011). *Advanced mechanics of materials and applied elasticity, 5th edition*. Pearson Education.